JOURNAL OF AGRICULTURAL AND FOOD CHEMISTRY

Microsomal Hydroxylation and Glucuronidation of [6]-Gingerol

ERIKA PFEIFFER, FRANZISKA F. HEUSCHMID, STEFAN KRANZ, AND MANFRED METZLER*

Institute of Applied Biosciences, Chair of Food Chemistry, University of Karlsruhe, P.O. Box 6980, D-76128 Karlsruhe, Germany

[6]-Gingerol is the major pungent principle of ginger and frequently is ingested with various condiments and nutritional supplements. We report here that incubation of [6]-gingerol with NADPH-fortified rat hepatic microsomes gave rise to eight metabolites, which were tentatively identified by GC-MS analysis as two products of aromatic hydroxylation as well as the diastereomers of two aliphatic hydroxylation products and the diastereomers of [6]-gingerdiol. Hepatic microsomes from rats and humans fortified with UDPGA glucuronidated [6]-gingerol predominantly at the phenolic hydroxyl group, but small amounts of a second monoglucuronide involving the aliphatic hydroxyl group were also identified by LC-MS/MS analysis. Human intestinal microsomes formed the phenolic glucuronide only. Supersomes containing human UGT1A1 and 1A3 exclusively generated the phenolic glucuronide, albeit with very low activities, whereas UGT1A9 catalyzed the specific formation of the alcoholic glucuronide and UGT2B7 the predominant formation of the phenolic glucuronide with high activities. Our study indicates a rather complex metabolism of [6]-gingerol, which should be taken into consideration for the multiple biological activities of this compound.

KEYWORDS: [6]-Gingerol; rat liver microsomes; hydroxylated metabolites; glucuronide; human UGT.

INTRODUCTION

Ginger, the rhizome of *Zingiber officinale* Roscoe (Zingiberaceae) is widely used as a common condiment for a variety of foods and beverages. In addition, crude or processed ginger has been employed in traditional oriental medicine for the treatment of many ailments (*1*). More recently, various extracts of ginger have appeared on the market as nutritional supplements. Ginger contains numerous biologically active constituents including the main pungent principles, the gingerols, among which [6]-gingerol (5-hydroxy-1-(4′-hydroxy-3′-methoxyphenyl)-3-decanone) is the major compound (**Figure 1**). Other gingerols share the aromatic ring and aliphatic 3-keto-5-hydroxy moiety but have longer alkyl chains at C-5.

Despite their frequent ingestion with food items or for medical reasons, very little is known about the metabolic fate of gingerols. In an in-vitro study with the postmitochondrial supernatant of rat liver homogenate fortified with a NADPH-generating system, [6]-gingerol was found to be reduced at the keto group to yield [6]-gingerdiol (*2*). This was confirmed in a later study, in which another metabolite was identified as 9-hydroxy-[6]-gingerol (*3*). Fortification of the rat liver postmitochondrial supernatant with UDPGA gave rise to the formation of one glucuronide, which was also detected in the bile of bile-duct-cannulated rats after oral administration of [6]-gingerol (*3*). In the urine of intact rats dosed with [6]-gingerol by gastric intubation, several metabolites with a shortened alkyl chain, for example, ferulic acid and vanillic acid, were identified (*3*). As their formation was markedly decreased after gut sterilization, these metabolites were probably generated by intestinal bacteria (*3*).

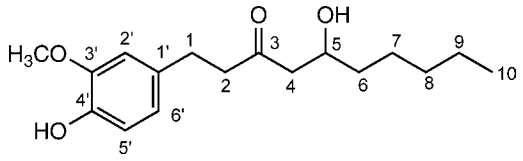

Figure 1. Chemical structure of [6]-gingerol.

Because [6]-gingerol offers several sites for aliphatic and aromatic hydroxylation, the aim of the present study was to clarify whether any products other than 9-hydroxy-[6]-gingerol are formed in rat liver microsomes. Moreover, the glucuronidation of [6]-gingerol, which may take place at the aliphatic or aromatic hydroxyl group, was studied in detail.

MATERIALS AND METHODS

Chemicals, Animals, and Cell Fractions. Racemic [6]-gingerol, prepared by chemical synthesis, was purchased from Dalton Pharma Services (Toronto, Ontario, Canada) and had a purity of >99% according to HPLC analysis. $NADP^+$, UDPGA, other chemicals and reagents, and β-glucuronidase (type B-1 from bovine liver) were obtained from Sigma/Aldrich/Fluka (Taufkirchen, Germany). HPLC-grade acetonitrile was from Carl Roth Co. (Karlsruhe, Germany).

Male Sprague−Dawley rats were purchased from Harlan Winkelmann GmbH (Borchen, Germany). Animals were kept under a 12-h

* To whom correspondence should be addressed. Tel: +49-721-6082132. Fax: +49-721-6087255. E-mail: manfred.metzler@chemie.uni-karlsruhe.de.

10.1021/jf062235l CCC: $33.50
Published on Web 10/13/2006

light/dark cycle and received water and commercial lab chow ad libitum. The livers of untreated male rats with 200−300-g weight and the liver of a 63-year-old white male (kindly provided by Dr. J. Weymann, former Knoll AG, Ludwigshafen, Germany) were used for the preparation of hepatic microsomes as described previously by Lake (*4*). Protein concentrations were measured according to Bradford (*5*) with bovine serum albumin as standard. The concentration of active cytochrome P450 was determined by the method of Omura and Sato (*6*).

Human intestinal microsomes and supersomes, that is, microsomes from insect Sf-9 cells infected with a baculovirus strain containing the cDNA of human UGT1A1, 1A3, 1A9, or 2B7, were from Gentest (Woburn, MA).

Microsomal Incubations. Oxidative in-vitro metabolism of [6]-gingerol was studied by incubating microsomes (1 mg of microsomal protein/mL) with 50−100 μM substrate dissolved in DMSO (final concentration 0.5−1%) and a NADPH-generating system (0.9 U isocitrate dehydrogenase, 9.4 mM isocitrate, 1.21 mM $NADP^+$, and 4.3 mM magnesium chloride) in a final volume of 1 mL, in 0.1 M phosphate buffer pH 7.4. After preincubation for 5 min at 37 °C, the NADPH-generating system was added, and the mixture was incubated for 40 min at 37 °C. Subsequently, the incubation mixture was extracted with 3 × 0.5 mL of ethyl acetate, and the extract was evaporated to dryness. The residue was dissolved in 50 μL of methanol for HPLC analysis. Control incubations were carried out with heat-inactivated microsomes, or with intact microsomes but without a NADPH-generating system.

In-vitro glucuronidation of [6]-gingerol and 4-(trifluoromethyl)-umbelliferone was carried out in a total volume of 0.2 mL of 0.1 M phosphate buffer, pH 7.4, containing 0.05 mg of hepatic or intestinal microsomal protein, or in 0.2 mL of 50 mM tris/chloride buffer, pH 7.5, containing 0.015 mg of supersome protein. In a typical incubation, the enzyme protein was first mixed with 25 μg of alamethicin in about 50 μL of buffer and placed on ice for 15 min. Subsequently, magnesium chloride (final concentration 10 mM), the β-glucuronidase inhibitor saccharolactone (5 mM), and [6]-gingerol (50−100 μM) dissolved in DMSO (final concentration 0.5−1%) were added, and the mixture was preincubated for 5 min at 37 °C. The reaction was initiated by adding UDPGA (4 mM) and terminated after 15−35 min by adding 25 μL of 20% aqueous trichloroacetic acid. After neutralization with 25 μL of 1 M aqueous sodium hydroxide, precipitated proteins were sedimented by centrifugation (5 min at 1000*g*) and the supernatant was analyzed by HPLC. Control incubations were carried out without UDPGA. Glucuronides were quantified through their absorbance, assuming that they have the same molar extinction coefficients as their aglycones. In some experiments, saccharolactone was omitted, and an aliquot of the incubation mixture was mixed with an equal volume of 0.15 M acetate buffer, pH 5.0, containing 1000 U of β-glucuronidase and incubated for 2 h at 37 °C prior to precipitation of proteins and HPLC analysis.

HPLC Analysis. A Beckman system equipped with a binary pump, a photodiode array detector, and 32 Karat 7.0 software for data collection and analysis was used. Separation was carried out on a 250 × 4.6-mm-i.d., 5-μm, reversed-phase Luna C8 column (Phenomenex, Torrance, CA). Solvent A was deionized water adjusted to pH 3.0 with formic acid, and solvent B was acetonitrile. A linear solvent gradient was used, with solvent A changing from 70 to 30% between the time of injection and 35 min, from 30 to 0% between 35 and 36 min, and from 0 to 30% between 36 and 41 min. The flow rate was 1 mL/min, and the detector was set to 280 nm. For further analysis by GC-MS, fractions of the NADPH-fortified microsomal incubations were collected, the acetonitrile removed with a rotary evaporator, and the remaining aqueous phases extracted with ethyl acetate. For LC-MS analysis of the glucuronides, HPLC fractions of the UDPGA-fortified incubations were first concentrated under reduced pressure and the aqueous phases subsequently acidified with 0.7 M glycine/chloride buffer, pH 1.2, and extracted with ethyl acetate.

GC-MS Analysis. A Finnigan GCQ capillary gas chromatograph equipped with a 30-m × 0.25-mm-i.d., 0.25-μm, 5% phenylmethyl MDN-5S fused-silica column (Supelco, Bellefonte, PA) and coupled to an ion-trap detector was operated with electron impact (EI) ionization at 70 eV (Thermo Finnigan, Austin, TX). Oven temperature was programmed from 60 (1-min hold) to 290 °C (10-min hold) at a rate of 15 °C/min. Temperatures of injector, transfer line, and ion source were 275, 275, and 250 °C, respectively. Samples (1-μL) dissolved in *N*,*O*-bis(trimethylsilyl)trifluoroacetamide were splitlessly injected with helium as carrier gas with a column pressure of 83 kPa. Mass spectra were scanned from *m*/*z* 50 to 650 at a rate of 0.5 s/scan.

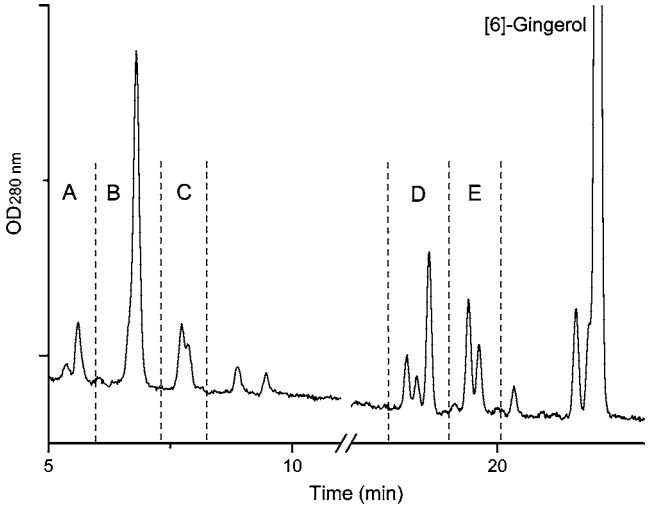

Figure 2. HPLC profile of the extract from the incubation of [6]-gingerol with NADPH-fortified rat liver microsomes. Fractions A–E were collected for subsequent GC-MS analysis.

LC-MS/MS Analysis. A Finnigan LCQ ion trap equipped with an ESI interface (negative mode) and operated by XCalibur version 1.0 software was used for MS^n experiments. Separations were achieved on a 150 × 2.0-mm-i.d., 5-μm, reversed-phase Luna C18(2) column (Phenomenex) equipped with a 4 × 2.0-mm guard column with the same material. Solvent A was deionized water acidified with 0.1% acetic acid, and solvent B was acetonitrile. A linear solvent gradient was used, with solvent B changing from 0 to 100% within 30 min after injection, followed by isocratic elution with 100% B for 5.0 min, restoration of the initial mobile-phase composition within 1 min, and column equilibration for 4.0 min, resulting in a total run time of 40.0 min. The flow rate was 300 μL/min, and the injection volume was 10 μL. The needle voltage of the ESI interface was set at −5.0 kV for negative ion mode, the sheath gas flow was 50 (arbitrary units), the temperature of the capillary was 200 °C, and the capillary voltage was −4 V. The automatic gain control of the ion trap was set to 5×10^7, with a maximum injection time of 200 ms. The window for the precursor ion selection was 1.0 mass unit. Nitrogen was used as vaporizer gas, while helium was used as damping and collision gas at a pressure of 0.1 Pa. Full-scan mass spectra were acquired over the mass range *m*/*z* 50−1000. For MS/MS investigation, the ions were isolated in the ion trap and collisionally activated with different collision energies (CE) to find the optimal CE for a distinct fragmentation. A CE of the LCQ is set using a scale of 0−100%. This adjusted value corresponds with 30% of the available 5-V peak-to-peak of resonance excitation radio frequency voltage. MS/MS spectra were acquired over the mass range *m*/*z* 150−1000.

RESULTS AND DISCUSSION

Metabolism in Rat Hepatic Microsomes Fortified with NADPH. Microsomes from the livers of male Sprague−Dawley rats were incubated with [6]-gingerol in the presence of a NADPH-generating system and subsequently extracted with ethyl acetate. Analysis of the extract by reversed-phase HPLC revealed the presence of at least eight peaks which eluted earlier than [6]-gingerol and which were not observed in control experiments with heat-inactivated microsomes or in the absence of the NADPH-generating system (**Figure 2**). For structure elucidation, the HPLC eluate was collected in five fractions A−E as indicated in **Figure 2**, and each fraction was extracted with ethyl acetate. One aliquot of each extract was rechromato-

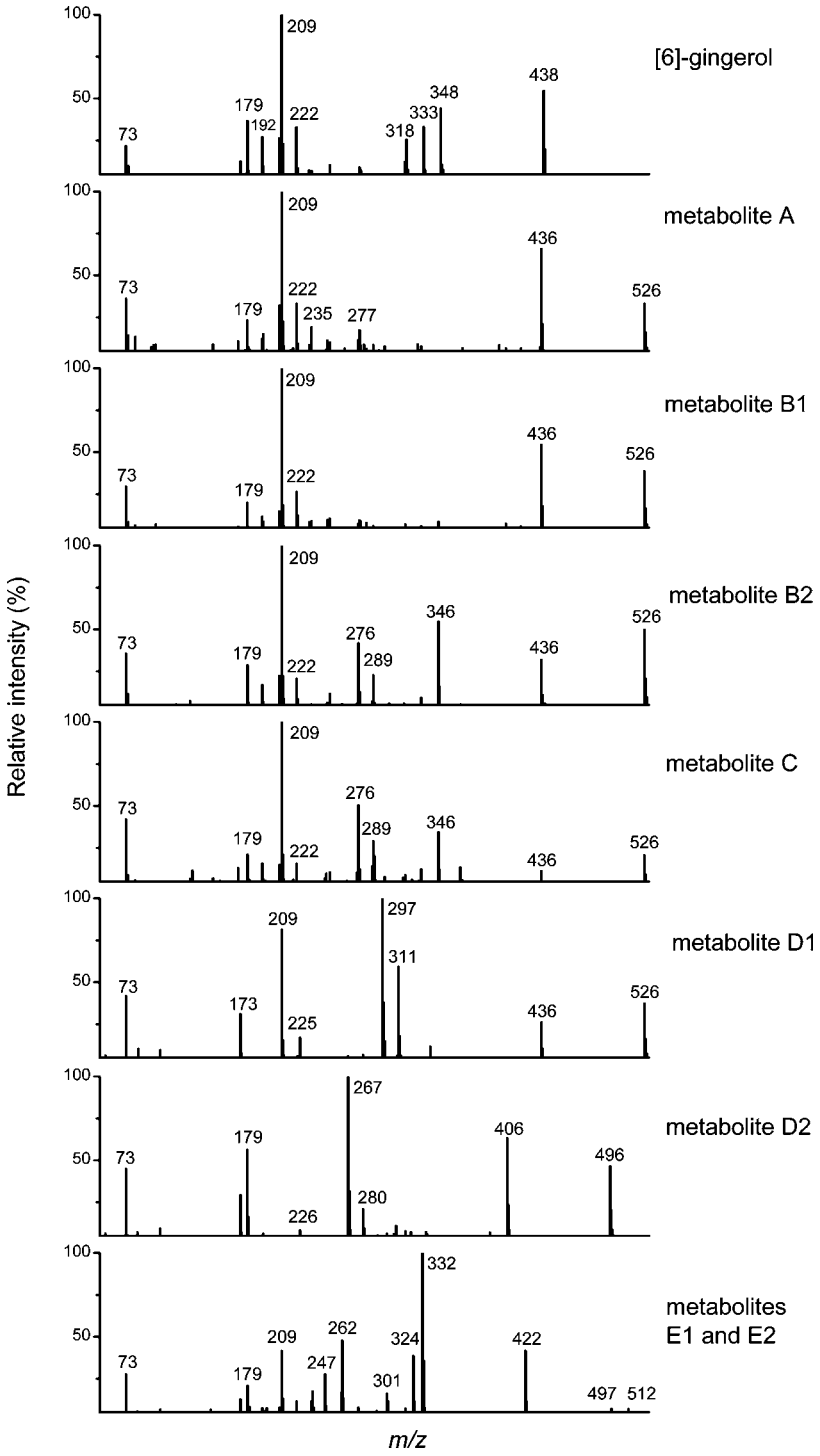

Figure 3. EI mass spectra of [6]-gingerol and its microsomal phase I metabolites after trimethylsilylation.

graphed by HPLC, and no peaks from neighboring fractions were detected in any of the collected fractions. The other aliquot was analyzed by GC-MS after trimethylsilylation. The HPLC rechromatograms indicated that the metabolites had survived the fractionation and processing without alteration (data not shown). The electron-impact mass spectra of the major metabolites and of [6]-gingerol are depicted in **Figure 3**.

A detailed discussion of the electron-impact mass spectra of trimethylsilyl derivatives of gingerols and related ginger constituents has been published by Harvey (*7*), who studied the fragmentation mechanisms by using various deuterated analogs. Our mass spectrum of [6]-gingerol (**Figure 3**, top) is virtually identical with that published by Harvey (*7*). Characteristic fragmentations are depicted in **Figure 4**. The fragmentation of the molecular ion at *m*/*z* 438 is dominated by a benzylic cleavage leading to the base peak at *m*/*z* 209. Due to the neighboring methoxyl and trimethylsiloxyl groups at the aromatic ring, ethane is eliminated and the ion at *m*/*z* 179 is obtained. A second prominent fragmentation involves the loss of trimethylsilanol from the aliphatic chain resulting in the ion at *m*/*z* 348. α-Cleavage at the keto group of this ion or the molecular ion leads to *m*/*z* 222. The loss of 30 amu (ethane) can also occur to the ions *m*/*z* 348 and 222, leading to *m*/*z* 318 and 192, respectively.

The most polar metabolite of [6]-gingerol, eluting in HPLC fraction A (**Figure 2**), gave rise to a mass spectrum with a

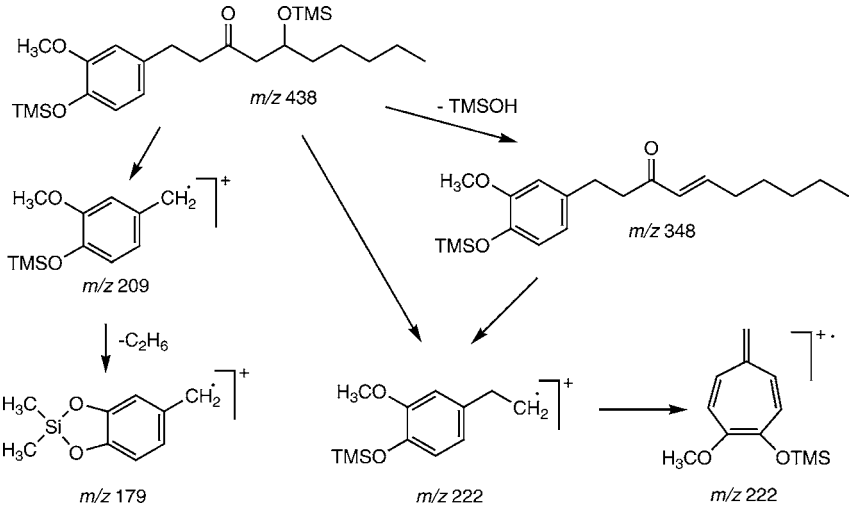

Figure 4. Major fragments in the EI mass spectrum of trimethylsilylated [6]-gingerol according to Harvey (*7*).

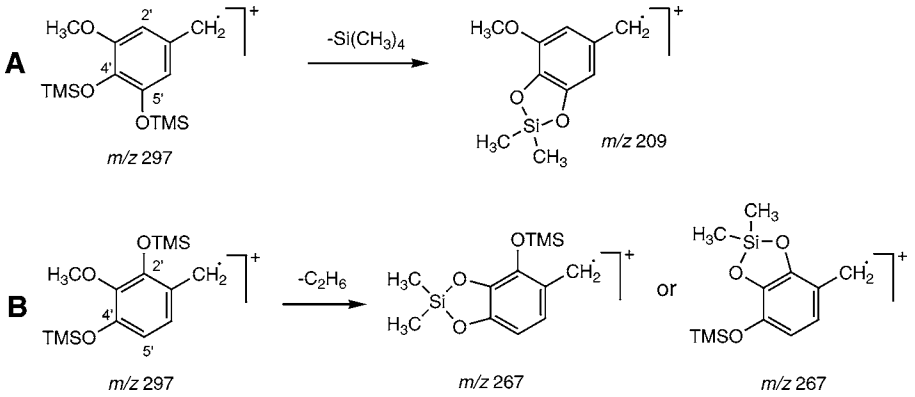

Figure 5. Proposed fragmentation of the aromatic ring system of [6]-gingerol after aromatic hydroxylation and trimethylsilylation, as observed in the EI mass spectra. (**A**) Metabolite D1; (**B**) metabolite D2.

molecular ion at *m*/*z* 526 in GC-MS (**Figure 3**). The increase in mass as compared to [6]-gingerol and the presence of the ions at *m*/*z* 179, 209, and 222, indicating an unchanged vanillic ring, suggests that metabolite A is a monohydroxylated [6]-gingerol with the additional hydroxyl group located at the aliphatic chain. The exact position of the new hydroxyl group cannot be determined with certainty from the mass spectrum. However, because there is only one elimination of trimethylsilanol, leading to *m*/*z* 436, the newly introduced hydroxyl group appears to be resistant to this type of fragmentation, implying its location at C-4 because elimination of two trimethylsilanols from this molecule would yield a ketene and should be unfavorable.

Fraction B, exhibiting one peak in HPLC analysis, contained two metabolites according to GC-MS analysis, which both had a molecular ion of *m*/*z* 526 (**Figure 3**). One of the mass spectra was identical with that of metabolite A from HPLC fraction A. Thus, metabolite B1 appears to be another diastereomer of 4-hydroxy-[6]-gingerol. The mass spectrum of the second metabolite of fraction B indicated the consecutive elimination of two trimethylsilanol molecules from the molecular ion, thereby leading to ions at *m*/*z* 436 and 346. This and the presence of an unchanged vanillic ring, indicated by the ions at *m*/*z* 179, 209, and 222, suggested one of the aliphatic carbons as the site of hydroxylation in metabolite B2. Again, the exact site could not be derived from the mass spectrum. HPLC fraction C exhibited one metabolite in GC-MS analysis, which had the same mass spectrum as metabolite B2 (**Figure 3**). It is therefore concluded that metabolites B2 and C represent diastereomers of a monohydroxylated [6]-gingerol carrying the second aliphatic hydroxyl group at any position between C-6 and C-10. It is conceivable that this metabolite is 9-hydroxy-[6]-gingerol previously reported by Nakazawa and Ohsawa (*3*).

HPLC fraction D contained three metabolites according to HPLC but exhibited only two prominent peaks in GC-MS analysis. The mass spectrum of metabolite D1 again had a molecular ion at *m*/*z* 526, indicating a monohydroxylated [6]-gingerol, and a fragment ion at *m*/*z* 436, indicating the elimination of one trimethylsilanol (**Figure 3**). However, the other fragment ions were quite different from those observed before. Of the diagnostic ions for the vanillic ring, *m*/*z* 179 and 222 were missing and 209 was not the base peak; instead, prominent ions were present at *m*/*z* 297 and 311. This strongly suggests that metabolite D1 carries the new hydroxyl group at the aromatic ring (**Figure 5**). As the ion at *m*/*z* 297 does not eliminate ethane to yield *m*/*z* 267 but tetramethylsilane to yield *m*/*z* 209, a catechol structure, that is, hydroxylation at C-5′, is proposed for this metabolite (**Figure 5A**). The second metabolite of HPLC fraction D also lacks two of the ions characteristic for the vanillic ring, that is, *m*/*z* 209 and 222; the base ion is at *m*/*z* 267 and other prominent ions are at *m*/*z* 406 and 496. These ions can be plausibly explained by assuming that [6]-gingerol has been hydroxylated at C-2′ of the aromatic ring next to the methoxyl group. After trimethylsilylation, this molecule would allow the elimination of ethane in two ways (**Figure 5B**), which would strongly favor this fragmentation and account for the absence of ions *m*/*z* 526, 436, and 297.

According to GC-MS analysis, HPLC fraction E contained two metabolites E1 and E2, which had identical mass spectra

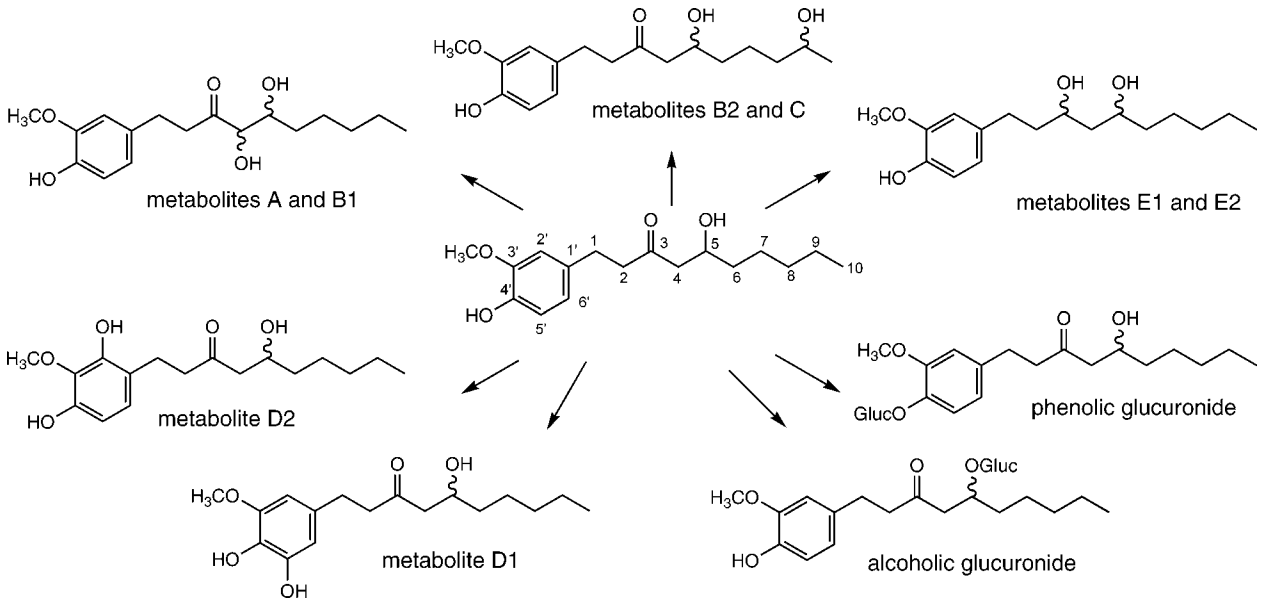

Figure 6. Proposed pathways in the in-vitro metabolism of [6]-gingerol.

Table 1. Glucuronidation of [6]-Gingerol ([6]-G) and 4-(Trifluoromethyl)-umbelliferone (TFMU) by Microsomes from Various Sources and by Supersomes Expressing Human Hepatic UGT Isoforms[a]

	proportion of glucuronide (%)		enzymatic activity (pmol/min/mg protein)	
enzyme	alcoholic	phenolic	for [6]-G	for TFMU
rat hepatic microsomes	13	87	32000	59000
human hepatic microsomes	5	95	13000	48000
human intestinal microsomes	0	100	86000	20000
UGT1A1	0	100	91	870
UGT1A3	0	100	230	840
UGT1A9	100	0	12000	11100
UGT2B7	8	92	88000	3000

[a] The substrate concentration was 50 μM, and the results are the mean of two or more independent experiments.

with molecular ions at *m*/*z* 512 and two successive eliminations of trimethylsilanol to give ions at *m*/*z* 422 and 332 (**Figure 3**). These mass spectra can best be explained by assuming the structure of [6]-gingerol with a reduced keto group, that is, [6]-gingerdiol. Our mass spectrum displays the same fragment ions as the spectrum of gingerdiol published by Harvey (*7*), although the relative intensities are different, which may be explained by the lower electron energy of 25 eV used by Harvey as compared to 70 eV in our studies. Therefore, we postulate that the metabolites E1 and E2 are diastereomers of [6]-gingerdiol.

In summary, our study has provided preliminary evidence for the formation of two aromatic hydroxylation products, two aliphatic hydroxylation products with two diastereomers each, and two diastereomers of [6]-gingerdiol in microsomal incubations of [6]-gingerol (**Figure 6**). However, it should be emphasized that the proposed structures are essentially based on mass spectrometry, and further studies, in particular by NMR spectroscopy, are clearly needed for confirmation. As the only mammalian metabolites of [6]-gingerol reported to date are [6]-gingerdiol and 9-hydroxy-[6]-gingerol (*3*), our study has clearly shown that the mammalian metabolism of [6]-gingerol is more complex than previously thought.

In-Vitro Glucuronidation of [6]-Gingerol. Glucuronidation of [6]-gingerol has previously been reported in the rat in vivo and in vitro (*3*). However, the exact structure of the glucuronide has not been determined, and no information is available on the isoforms of UGT involved in gingerol glucuronidation. In our study, [6]-gingerol was incubated with hepatic microsomes from male Sprague−Dawley rats in the presence of UDPGA and the incubation mixture subsequently analyzed by HPLC. In addition to unreacted [6]-gingerol eluting at 22.7 min, two more polar peaks eluting at 13.1 and 14.7 min were observed, which were not present when the incubation mixture was treated with β-glucuronidase prior to HPLC, indicating that the two polar peaks are glucuronides. Analysis by LC-MS showed that both peaks exhibited parent ions at *m*/*z* 469 and are therefore monoglucuronides. However, a markedly different fragmentation of these parent ions was obtained upon MS/MS. Whereas glucuronide-1 (eluting at 13.1 min) exhibited a single fragment ion at *m*/*z* 193, glucuronide-2 (eluting at 14.7 min) gave rise to intense fragment ions at *m*/*z* 175 and 451. The fragment ion at *m*/*z* 175 most likely represents glucuronic acid, and the ion at *m*/*z* 451 remains after loss of water from the parent ion. As the latter fragmentation requires a free aliphatic hydroxyl group, is is proposed that glucuronide-2 carries the glucuronic acid moiety at the phenolic hydroxyl group (**Figure 6**). Therefore, glucuronide-1 is thought to represent an alcoholic glucuronide (**Figure 6**). In agreement with this notion is the fragment at *m*/*z* 193, which was also obtained by MS/MS of unconjugated [6]-gingerol. This ion presumably arises from cleavage of the bond between C-4 and C-5 of the gingerol molecule and should not be affected by glucuronidation of the alcoholic hydroxyl group.

The relative proportion of the aliphatic glucuronide-1 and the aromatic glucuronide-2 formed in rat liver microsomes from [6]-gingerol was about 13 and 87%, respectively, and remained almost constant when the total amount of glucuronide formation was modulated by variation of the concentrations of the substrate or protein or the incubation time (data not shown). With human hepatic microsomes, the ratio of the aliphatic to the aromatic glucuronide was even somewhat lower than with rat hepatic microsomes, and no aliphatic glucuronide of [6]-gingerol was obtained with human intestinal microsomes (**Table 1**). Of the three types of microsomes, those from human intestine exhibited the highest activity for the glucuronidation of [6]-gingerol (**Table 1**). For the model substrate 4-(trifluoromethyl)umbelliferone, rat and human hepatic microsomes had about equal

activity whereas the activity of human intestinal microsomes was markedly lower (**Table 1**).

In order to elucidate which isoforms of UGT are involved in the aromatic and aliphatic glucuronidation, [6]-gingerol was incubated with supersomes expressing four typical human liver UGT isoforms. The glucuronidation of 4-(trifluoromethyl)-umbelliferone was determined for comparison. As shown in **Table 1**, UGT1A1 and 1A3 generated exclusively the aromatic glucuronide, although with a rather low activity. In contrast, UGT1A9 formed specifically the aliphatic glucuronide with a markedly higher activity. The most active UGT isoform was UGT2B7, which mediated the preferential glucuronidation of the phenolic hydroxyl group. Notably, the activity of UGT2B7 was about 30-fold higher for [6]-gingerol than for 4-(trifluoromethyl)umbelliferone. In summary, our study has provided preliminary evidence that [6]-gingerol can be glucuronidated at the aromatic and aliphatic hydroxyl group and that the site of glucuronidation depends on the UGT isoform.

This study on the metabolism of [6]-gingerol in rat and human microsomes has revealed the formation of several new monohydroxylated products, including one metabolite with a catechol structure, which may be of toxicological significance. Nagabhusan et al. (*8*) have shown that [6]-gingerol exhibits mutagenic activity in the Ames *Salmonella* assay when postmitochondrial supernatant was included for metabolic activation. It is conceivable that the catechol of [6]-gingerol or a product of subsequent oxidation, for example, a semiquinone or quinone metabolite, represents the mutagenic agent. Further studies should now confirm the proposed structures by NMR spectroscopy and clarify whether the oxidative metabolites demonstrated in vitro are also formed in vivo in the rat and human. Moreover, the avid glucuronidation of [6]-gingerol observed with human intestinal microsomes and with UGT2B7 is of interest. The former could indicate an intestinal first-pass effect, whereas the latter might lead to interference with the glucuronidation of other substrates of UGT2B7, for example, the endogenous estrogen 17β-estradiol. UGT2B7 catalyzes the formation of estradiol-17-glucuronide, which is known to lower the flow of bile (*9*). The competitive inhibition of 17-glucuronidation of 17β-estradiol may be part of the stimulatory effect on bile secretion attributed to [6]-gingerol. Likewise, the importance of the oxidative and conjugative metabolites for the numerous other biological activities of [6]-gingerol should be addressed in further studies.

ABBREVIATIONS USED

CE, collision energy; EI, electron impact; NADP(H), nicotinamide dinucleotide phosphate, (reduced form); NMR, nuclear magnetic resonance; TMS, trimethylsilyl; UDPGA, uridine-5′-diphosphoglucuronic acid.

LITERATURE CITED

(1) Afzal, M.; Al-Hadidi, D.; Menon, M.; Pesek, J.; Dhami, M. S. Ginger: an ethnomedical, chemical and pharmacological review. *Drug Metab. Drug Interact.* **2001**, *18*, 159−190.

(2) Surh, Y. J.; Lee, S. S. Enzymic reduction of [6]-gingerol, a major pungent principle of ginger, in the cell-free preparation of rat liver. *Life Sci.* **1994**, *54*, PL 321−326.

(3) Nakazawa, T.; Ohsawa, K. Metabolism of [6]-gingerol in rats. *Life Sci.* **2002**, *70*, 2165−2175.

(4) Lake, B. G. Preparation and characterization of microsomal fractions for studies on xenobiotic metabolism. In *Biochemical Toxicology, A Practical Approach*; Snell, K., Mullach, B., Eds.; IRL Press: Oxford, U.K., 1987; pp 183−215.

(5) Bradford, M. M. A rapid and sensitive method for the quantitation of microgram quantities of protein utilizing the principle of protein-dye binding. *Anal. Biochem.* **1976**, *72*, 248−254.

(6) Omura, T.; Sato, R. The carbon monoxide-binding pigment of liver microsomes: I. Evidence for its hemoprotein nature. *J. Biol. Chem.* **1964**, *239*, 2370−2378.

(7) Harvey, D. J. The mass spectra of the trimethylsilyl derivatives of ginger constituents. *Biomed. Mass Spectrom.* **1981**, *8*, 546−552.

(8) Nagabhushan, M.; Amonkar, A. J.; Bhide, S. V. Mutagenicity of gingerol and shogaol and antimutagenicity of zingerone in Salmonella/microsome assay. *Cancer Lett.* **1987**, *36*, 221−233.

(9) Vore, M.; Liu, Y.; Huang, L. Cholestatic properties and hepatic transport of steroid glucuronides. *Drug Metab. Rev.* **1997**, *29*, 183−203.

Received for review August 3, 2006. Revised manuscript received September 5, 2006. Accepted September 6, 2006.

JF062235L